Ecosystems threatened by intensified drought with divergent vulnerability

Chen, Q.; Timmermans, J.; Wen, W.; Bodegom, P.M. van

Remote Sensing of Environment 289 (2023) 113512

Contents lists available at ScienceDirect

Remote Sensing of Environment

journal homepage: www.elsevier.com/locate/rse

Ecosystems threatened by intensified drought with divergent vulnerability

Qi Chen [a,*], Joris Timmermans [a,b,c], Wen Wen [a], Peter M. van Bodegom [a]

[a] Institute of Environmental Sciences (CML), Leiden University, Box 9518, 2300 RA Leiden, the Netherlands
[b] Virtual Laboratory and Innovation Centre (VLIC), Lifewatch ERIC, Science Park 904, 1098 XH Amsterdam, the Netherlands
[c] Institute for Biodiversity and Ecosystem Dynamics (IBED), University of Amsterdam, 1090 GE Amsterdam, the Netherlands

ARTICLE INFO

Edited by Jing M. Chen

Keywords:
Drought
Ecosystem vulnerability
Characteristics
Europe
Remote sensing
High resolution

ABSTRACT

Global climate change is projected to increase the severity and duration of droughts across many regions of the world, which could push ecosystems across their tipping points. To protect the most vulnerable ecosystems, it is critical to understand if ecosystems are likely to collapse rapidly or have a certain buffer capacity with aggravating drought (as characterized by their onset, duration and severity). However, such ecosystem vulnerability has been rarely characterized. Here, we present a novel, multi-faceted approach to quantify the ecosystem vulnerability and associated impacts of drought characteristics across different ecosystems at the continental-scale in Europe using high spatial and temporal resolution satellite data. We observed substantially different vulnerabilities across ecosystems where the vegetation damage increases with earlier, longer and more intense droughts. In particular, irrigated croplands are under prominently high risk when facing intensified droughts with the shortest delay in response to drought (0.67 times that of other ecosystems) and a fast increase in damage to drought (1.27 times that of other ecosystems). Mixed forests have a prominently low vulnerability in terms of a notably slow increase in damage to drought (0.67 times that of other ecosystems) and a relatively long response time (longer than over half ecosystems). Moreover, the vulnerability of most ecosystems largely increases with increasing drought severity. Consequently, vegetation tends to succumb more quickly to intensified droughts. Our multi-faceted approach to ecosystem vulnerability characterization indicates that under future intensified droughts in the 21st century, the functioning of a vast range of ecosystems will be threatened.

1. Introduction

Droughts, together with other climate disasters, are considered one of the biggest threats to humankind, in terms of likelihood and impacts (World Economic Forum, 2018). Droughts provide tremendous threats to ecosystem structures (Batllori et al., 2020; Senf et al., 2020; Stovall et al., 2019) and functioning (Anderegg et al., 2013; Ciais et al., 2005), and the provisioning services (Gupta et al., 2020; Kang et al., 2021; Verschuur et al., 2021) and regulating services (Anderegg et al., 2019; Phillips et al., 2009; Reichstein et al., 2013) that our ecosystems offer (Millar and Stephenson, 2015). Droughts are projected to be more prolonged and extreme over the 21st century (Field et al., 2012), especially in Europe (Naumann et al., 2021; Samaniego et al., 2018). These projected intensified droughts are likely to have profound impacts on the structuring and functioning of Earth's ecosystems (Seddon et al., 2016) and may push ecosystems to their physiological limits (Allen et al., 2010; Stovall et al., 2019). Facing these deteriorating droughts (characterized by e.g., earlier onset, increasing duration and severity), understanding if ecosystems are likely to destabilize rapidly or have a certain buffer capacity is therefore becoming increasingly important for ecosystem service provision and risk management policies. For this, we need to quantify such ecological vulnerability to drought and prioritize ecosystems that are most susceptible to drought.

In the past decade, the scientific community has explored ecosystem vulnerabilities using multiple remote sensing datasets that allow for large-scale and long-term monitoring (AghaKouchak et al., 2015). Most recent studies have focused on statistical frameworks to evaluate the vulnerability of vegetation (Páscoa et al., 2018; Xu et al., 2018; Zhang et al., 2017). Specifically, many studies estimated temporal correlations between drought indexes and vegetation indexes (Ding et al., 2020; Gouveia et al., 2017; Ji and Peters, 2003), such as utilizing commonly used drought indexes like the Standardized Precipitation Evapotranspiration Index (SPEI) (Vicente-Serrano et al., 2010), Standardized Precipitation Index (SPI) (McKee et al., 1993) and Palmer Drought Severity Index (PDSI) (Palmer, 1965) and vegetation indexes like the Normalized Difference Vegetation Index (NDVI), Vegetation Condition Index (VCI)

* Corresponding author.
E-mail address: q.chen@cml.leidenuniv.nl (Q. Chen).

https://doi.org/10.1016/j.rse.2023.113512
Received 2 September 2022; Received in revised form 17 January 2023; Accepted 14 February 2023
Available online 1 March 2023

(Kogan, 1995) and Enhanced Vegetation Index (EVI) (Huete et al., 2002). By linking drought to vegetation indexes by temporal correlation analysis, studies have evaluated effects of long-term climate conditions on vegetation. However, such analyses failed to distinguish among different aspects of drought (i.e. onset, duration and severity) and potentially differential responses in vegetation damage. Thus, they can hardly reveal how damage may increase with specific deteriorating drought characteristics (i.e. ecosystem vulnerability).

Ecosystem damage to drought can be explicitly characterized by damage timing, damage duration and damage severity (Chen et al., 2022). Each of these attributes may have a different sensitivity to the corresponding drought characteristics. Understanding this multi-faceted nature of vulnerability is a prerequisite for predicting the damage in ecosystems facing future drought events. To be able to couple multiple attributes of drought and vegetation damage episodes in different ecosystems, higher spatial and temporal resolution data is required (Kuenzer et al., 2014), whereas meteorological data applied in previous European-wide studies was limited to a monthly-25 km resolution (Muffler et al., 2020; Sun et al., 2018). Up to now, approaches to quantify such multi-faceted vulnerability of different ecosystems across large scale have not been developed.

In this work, we developed a quantitative understanding of multiple facets of drought vulnerability of ecosystems using three drought characteristics (onset, duration, severity) across 21 ecosystems with high resolution data at the continental scale of Europe's ecosystems. Our research addressed the following questions: (1) What are the spatial and temporal patterns of drought and ecosystem response characteristics?, (2) How do different ecosystems respond to earlier, longer and more intense droughts?, and (3) How does vulnerability vary within and between ecosystems with changing drought characteristics?

To answer these questions, we focused our efforts on the recent pan-European drought of 2018 using high spatial and temporal resolution remote sensing observations. We fused multiple precipitation products to produce a dataset with higher resolution than previous datasets (Chen et al., 2022). Combining this precipitation data with potential evapotranspiration (PET) data, the standardized precipitation index (SPEI) drought index was calculated across Europe for 2018 at a daily temporal resolution. In parallel, the vegetation damage was estimated on the basis of the standardized anomaly in leaf area index (LAI) as compared to 2004–2017 to quantify the impact on ecosystems. Instead of relating drought index (SPEI) directly to vegetation index (LAI), we coupled corresponding drought and ecosystem characteristics in terms of onset, duration and severity derived from these indexes. The relationships between these corresponding drought and ecosystem characteristics were analyzed. We find that ecosystems respond in different ways to earlier, longer and more intense droughts. This will allow estimating impacts of earlier, longer and severer droughts in the future (e.g., in terms of when the vegetation damage will start, how long this damage will last and the extent of this damage). Moreover, we show that ecosystem vulnerability increases disproportionally with an increase in drought severity. Thus, most ecosystems will be at risk by more intense droughts in the future.

2. Materials and methods

2.1. Data processing

An analytical framework has been constructed to quantify the ecosystem vulnerability across Europe utilizing drought and vegetation damage information data. For characterizing the drought event, daily SPEI-3 was calculated for 2018 on basis of the MARS precipitation data (from Agri4Cast of JRC) (Toreti, 2014) which was upscaled using the Meteosat Second Generation-Cloud Physical Properties (MSG-CPP) precipitation data (from the Royal Dutch Meteorology Institute, KNMI), and MODIS MOD16A2 PET data (Running et al., 2017) (from the United States Geological Survey, USGS) from 2004 to 2018. For more information regarding the SPEI product, refer to Chen et al. (2022).

To quantify the vegetation damage caused by drought, the Standardized Anomaly LAI (SALAI) was calculated with the GEOV2 LAI data (from the Copernicus Global Land Service) (Copernicus Service Information, 2019) from 2004 to 2018. This validated LAI data product is available (https://land.copernicus.eu/global/products/lai) each 10 days at 1 km resolution. We calculated SALAI based on Eq. (1) (Chen et al., 2022):

$$SALAI(t) = \frac{LAI(t) - \overline{LAI}(t)}{\sigma(t)} \quad (1)$$

Where $SALAI(t)$ is the SALAI at time t, $LAI(t)$ is the LAI value at time t, $\overline{LAI}$ is the temporal mean of LAI at time t over 15 years, and σ is the standard deviation of LAI.

Considering that the direct damage caused by fire to vegetation will affect our analysis of drought response, based on the 2017–2018 monthly fire data from NASA Earth Observations (https://neo.gsfc.nasa.gov/), we eliminated the (frequent fire) areas where the sum of fires in the 24 months is greater than the 95th percentile. Pixels with maximum LAI values in 2017–2018 lower than 0.4 were removed and pixels with values less than the 0.2th percentile of vegetation damage severity (indicated by severity calculated based on SALAI) were also removed. These thresholds were chosen to remove interference factors while keeping as many pixels as possible. Separate data filters were built based on above principles. If one or more factors exceeded its threshold, the pixel was removed.

To investigate how vulnerability changes not only spatially but also per ecosystem type, we used the Copernicus Climate Change Service (C3S) 2018 landcover (LC) map (C3S, 2019), which utilizes a consistent classification as the Land Cover Climate Change Initiative (CCI) from the European Space Agency (ESA). This open available map (https://maps.elie.ucl.ac.be/CCI/viewer/) provides high resolution (300 m) validated landcover data across Europe. The dataset was used to classify ecosystems in our research area (Supplementary Table S1).

All data were reprojected to wgs84 and resampled to a common grid with 0.005 degrees resolution. Only droughts during the year which contained the vegetation life cycle were considered. Therefore, we calculated the drought index SPEI and the vegetation damage index SALAI from 2017.09.20 to 2018.09.19 for the vegetation whose phenology correspondingly spanned two years in the Mediterranean region. In other regions, indexes of year 2018 were used to match the life cycle of vegetation. We did not further constrain data selection as we observed that constraining data to the growing season in croplands hardly impacted the results.

2.2. Drought and vegetation damage characteristics

The onset, duration and severity of drought were calculated based on the drought index SPEI. We used −0.5 of SPEI as the upper-threshold for drought. Then, the total number of days at which SPEI values were lower than −0.5 was defined as drought duration, and the sum of these SPEI values was defined as drought severity. The drought event with the longest duration was identified and its onset date was calculated. In addition, the onset, duration and severity of vegetation damage were calculated according to the same method based on SALAI. Vegetation damage was recognized as SALAI values lower than −1.

In order to understand at which stage of vegetation growth the drought event occurred, we converted the calculated drought onset date to onset stage through the following equation:

$$Drought\ onset\ stage = (Drought\ onset\ date - SOS)/(EOS - SOS) \quad (2)$$

In which SOS is the Start Of Season date and EOS the End of Season date. Drought onset stage represents the stage in the growing season where the drought event occurred and ranges from 0 to 1. The SOS and EOS of vegetation were calculated by software TIMESAT based on LAI

data. The onset conversion calculation was also performed by using the SOS and EOS from Modis phenology product (Zhang et al., 2020) (https://doi.org/10.5067/VIIRS/VNP22Q2.001). These onsets derived from Modis were similar to that from TIMESAT (Jönsson and Eklundh, 2002, 2004) (Supplementary Fig. S1). The onset of the vegetation damage event also underwent the same conversion.

2.3. Data analysis

The spatio-temporal patterns of drought and vegetation damage and the associated ecosystem vulnerability across Europe were quantified: First, to exclude interference from other factors, only those pixels exposed to drought in 2018 were considered in the analysis. To exclude damage caused by other factors, those pixels with significant negative Pearson correlations between SALAI and SPEI were excluded from the analysis except when the negative correlations were caused by the absence of damage during drought. Second, contour plots were made based on Gaussian kernel densities using the drought and vegetation damage characteristics. Third, based on drought and vegetation damage characteristics, standardized major axis (SMA) estimation was used as an estimate of vegetation vulnerability, using the SMATR package (Standardized Major Axis estimation and Testing Routines) (Warton et al., 2012) in R. Slopes of the best fitted lines between drought and vegetation damage characteristics were provided by SMA, which was used to quantify vegetation vulnerability.

To reduce the influence of outliers on line fitting, a robust SMA was fitted using Huber's M estimation. Due to the operating limitations of this calculation method and the vast number of pixels, we resampled the samples at equal intervals. The SMA slopes were quantified and compared, which allows us to more objectively investigate the variation in responses to drought between different ecosystem types. The similarity between the slopes of these different ecosystem types was analyzed using multiple posthoc comparisons by the SMATR package of the SMA fit. Similar slopes were grouped. Insignificant slopes ($P > 0.05$) and slopes with R-squared <0.01 were considered zero. Because of the finite spatial distribution range and drought severity range of broad-leaved evergreen forests and Lichens and mosses, the analysis of their slopes was limited.

To further evaluate the vulnerability of ecosystems in terms of damage to varying drought severity, we divided vegetation damage severity into 5 levels and drought severity into 6 levels ($0 \sim -600$). Vegetation damage severity of ecosystems was first normalized to a range of 0–1 using min-max normalization. Then the percentage of observations that falls within one damage level was calculated for each drought severity level.

We focus our analysis on severity-severity slopes to express the damage vulnerability of different ecosystem types. Basically, the larger the slope, the greater the vegetation damage with increasing drought severity, and the more vulnerable the vegetation is. To accurately estimate how damage vulnerability changes with drought severity, the

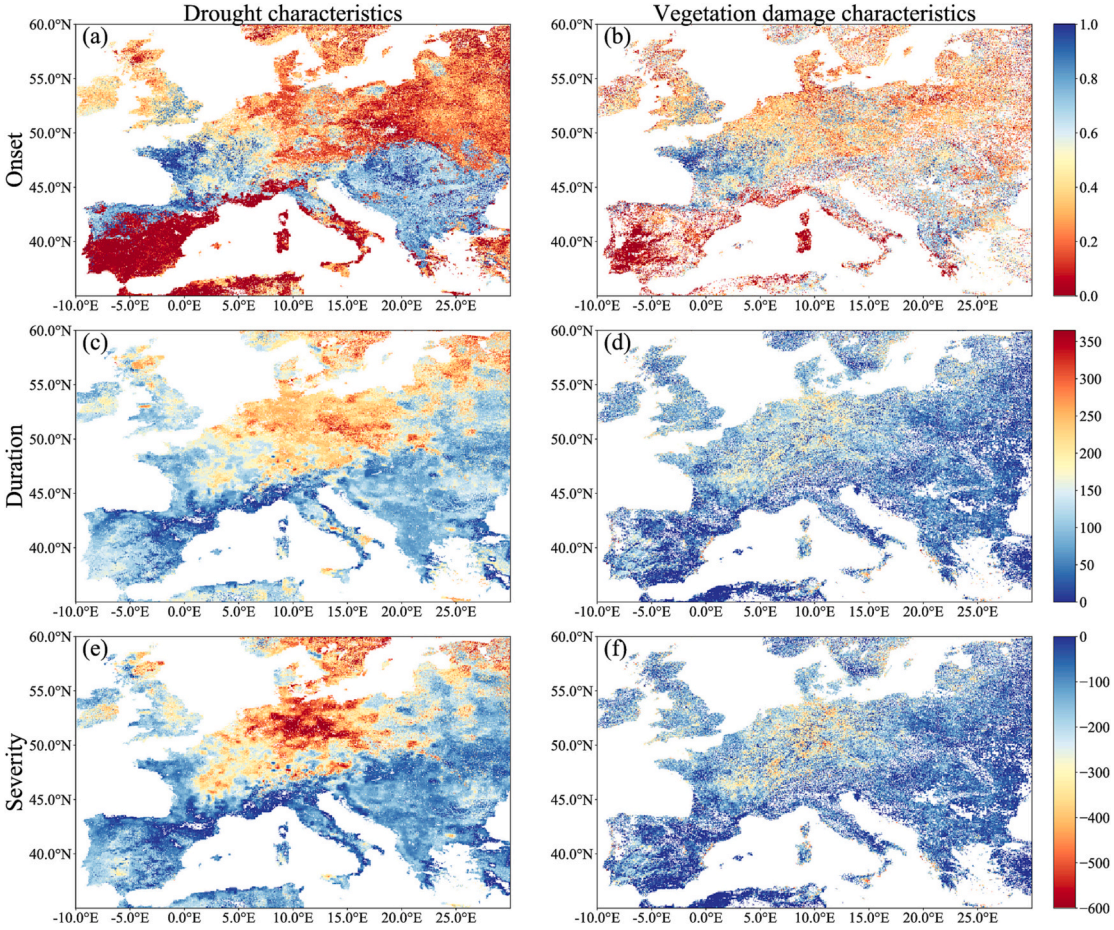

Fig. 1. Spatial patterns of drought and vegetation damage characteristics. a, Onset of longest drought based on the 3-month SPEI in Europe. **b**, Onset of vegetation damage based on SALAI. Onset was converted to the stage in the growing season where the anomalous event occurred (e.g. stage 0 and 1 means start and end of the growing season, respectively). **c**, **d**, Drought duration and vegetation damage duration (measured in days). **e**, **f**, Drought severity and vegetation damage severity (measured as the sum severity of anomaly SPEI or SALAI values - as defined in methods - over the full duration of the drought or damage). Pixels without drought were not shown for drought duration and severity. Drought and vegetation damage characteristics of different ecosystem types can be found in Supplementary information (Supplementary Fig. S3).

relationship between vegetation damage severity and drought severity was fitted by a generalized additive model (GAM) using the mgcv package (Wood, 2011) in R (Supplementary Fig. S2). The smooth basis dimension in GAM was limited to 4 to avoid model overfitting. Subsequently, the first derivatives (slopes) were derived from the fitted GAM models of each ecosystem type. The same process was applied to onset-onset and duration-duration slopes.

3. Results

3.1. Variability in spatial distribution of drought and vegetation damage characteristics in Europe

The spatial distribution and temporal dynamics of drought and vegetation damage characteristics of the severe drought of 2018 (unprecedented in the past 2110 years (Büntgen et al., 2021)) differed for different parts of Europe (Fig. 1). Central Europe experienced the severest drought, whereas southern Europe experienced milder drought (left panel of Fig. 1). In particular, the drought in the Netherlands, Belgium, Germany, Poland and Czechia occurred early (earlier than stage 0.3 of the growing season), and lasted longer (longer than 200 days) causing a more severe event. At the western coast of the Mediterranean (such as south Spain and south Portugal) the drought also started at an early stage of the growing season (earlier than stage 0.2), however with a shorter duration (shorter than 100 days), and the overall severity of the drought was much less. In general, patterns of vegetation damage were consistent with the spatial distribution of drought characteristics, though with higher spatial heterogeneity (right panel of Fig. 1). Most onsets of vegetation damage showed abnormal development at the peak stage of its growing season. Similar to the drought duration and severity, we observed longer affected periods and more severe damage of vegetation in the central and northeastern France, the Netherlands, Belgium, Germany, Czechia and western Poland.

3.2. Ecosystems respond differently to earlier, longer and more intense droughts

The relationships between these high-resolution drought and vegetation damage characteristics reflect the ecosystem responses to water stress from multiple aspects (delay time, suffering period and response intensity), which will allow predicting ecosystem responses to future earlier, longer and more intense droughts. We derived the slopes between the onset-onset, duration-duration and severity-severity by using standardized major axis (SMA) estimation to indicate ecosystem vulnerability. If with an increasing drought duration and severity the vegetation damage is less long and less severe, this will translate in lower slopes (Supplementary Fig. S5 and Fig. S6), and therefore indicates a lower vulnerability. In contrast, a higher onset-onset slope indicates a longer delay time of the vegetation damage, and hence a lower drought vulnerability. The combination of these three aspects reflects vegetation strategies facing drought.

Using the onset-onset slopes, we found that the time when vegetation started to be damaged by the water shortage, depends on the onset of the drought events. Specifically, we found a linear pattern (Supplementary Fig. S4) between the onsets of vegetation damage and drought with significant correlations (R^2 ranging 0.06 to 0.41, with an average of 0.21, $P < 0.05$), indicating that almost all ecosystem types vegetation damage onsets followed the drought onsets. This may imply that with an earlier drought onset in the future, ecosystems would also be damaged earlier.

Interestingly, this onset-delay (represented by the onset-onset slope) varies per ecosystem type (Fig. 2a), indicating different delays of vegetation for different ecosystems. For croplands, an onset-onset relationship was found with slopes <1, indicating that the crops responded quickly to drought and were already affected by water stress before the longest drought event had started. Among croplands, irrigated croplands showed the shortest delay time (with a slope of 0.68), while rainfed tree/shrub cover croplands showed the longest delay time (a slope close to 1). The response time of trees to drought showed a relatively long delay. Specifically, wetland ecosystems with tree cover showed the longest delay in drought onset (with a slope of 1.88), and needle-leaved deciduous forests also showed a long delay (with a slope of 1.23). The delays in the onset of vegetation damage in grasslands were between that of trees and crops.

Most of the vegetation showed an increased damage duration with an increase of drought duration (Supplementary Fig. S5). This suggests that with drought duration predicted to increase in the future (Samaniego et al., 2018), the duration of damage to the vegetation will also increase. However, ecosystems showed different vulnerabilities (as indicated by slopes) of damage duration with extending drought duration. We find that for forests the period of vegetation damage grew most slowly with an increase of drought duration, never exceeding the drought duration (slope < 1) (Fig. 2b). Among crops, the duration of vegetation damage also grew slowly with increasing drought duration in some types (slope < 1), while slope > 1 for irrigated croplands, rainfed tree/shrub cover croplands and mosaic natural vegetation/croplands. For grasslands, we find similar durations for drought and vegetation damage (slope ~ 1).

Severity-severity slopes (Fig. 2c) varied strongly across different ecosystem types, with forested ecosystems showing a relatively slow increase in damage with increasing drought severity (small slopes and low vulnerability) and crops having a relatively fast increase in damage (high slopes and high vulnerability). Specifically, we observed that mixed forests and needle-leaved evergreen forests both have a relatively low vulnerability to drought severity (with slopes of 0.54 and 0.59, respectively). Forests with mixed coniferous and broad-leaved trees were less vulnerable than simple coniferous or broad-leaved forests. Among crops, rainfed tree/shrub cover croplands, mosaic natural vegetation/croplands and irrigated croplands were the most vulnerable types, with slopes of 1.04, 1.01 and 0.99, respectively. Surprisingly, rainfed croplands and rainfed herbaceous croplands were found to be the least vulnerable types among the crops, with slopes of 0.71 and 0.70. In general, irrigated croplands were much more vulnerable than most rainfed croplands. The vulnerability of crops mixed with natural vegetation was also found to be higher than that of rainfed croplands and rainfed herbaceous croplands. Grasslands and mosaic vegetation were more vulnerable than most forests but less vulnerable than irrigated croplands. Among wetlands, systems with flooded shrub/herbaceous cover showed a relatively lower vulnerability than terrestrial grasslands and shrublands. Mosaic forests, in which trees and shrubs have a higher cover than herbaceous plants, were less vulnerable than mosaic grasslands, in which herbaceous cover dominates. The high proportion of trees and shrubs in mosaic forest/grassland seems to increase its drought resistance and thereby reduce its vulnerability. In contrast, in sparsely vegetated and rainfed croplands, tree/shrub cover seems to increase its vulnerability. Compared to herbaceous plants, trees or shrubs growing in areas with relatively harsh environments may increase the vulnerability of the ecosystem to drought. The low vulnerability of sparse herbaceous cover may be affected by the inaccurate detection in LAI variation induced by the low LAI values.

Evaluating the vegetation damage distribution across a range of drought severities (Fig. 3) provided more insights in ecosystem vulnerability. For example, the low vulnerability of mixed forests and needle-leaved evergreen forests was due to their low sensitivity of vegetation damage to increased drought severity and the high percentage of mild damage observations under severe drought. Closed broadleaved deciduous forest, needleleaved deciduous forest and flooded tree cover did

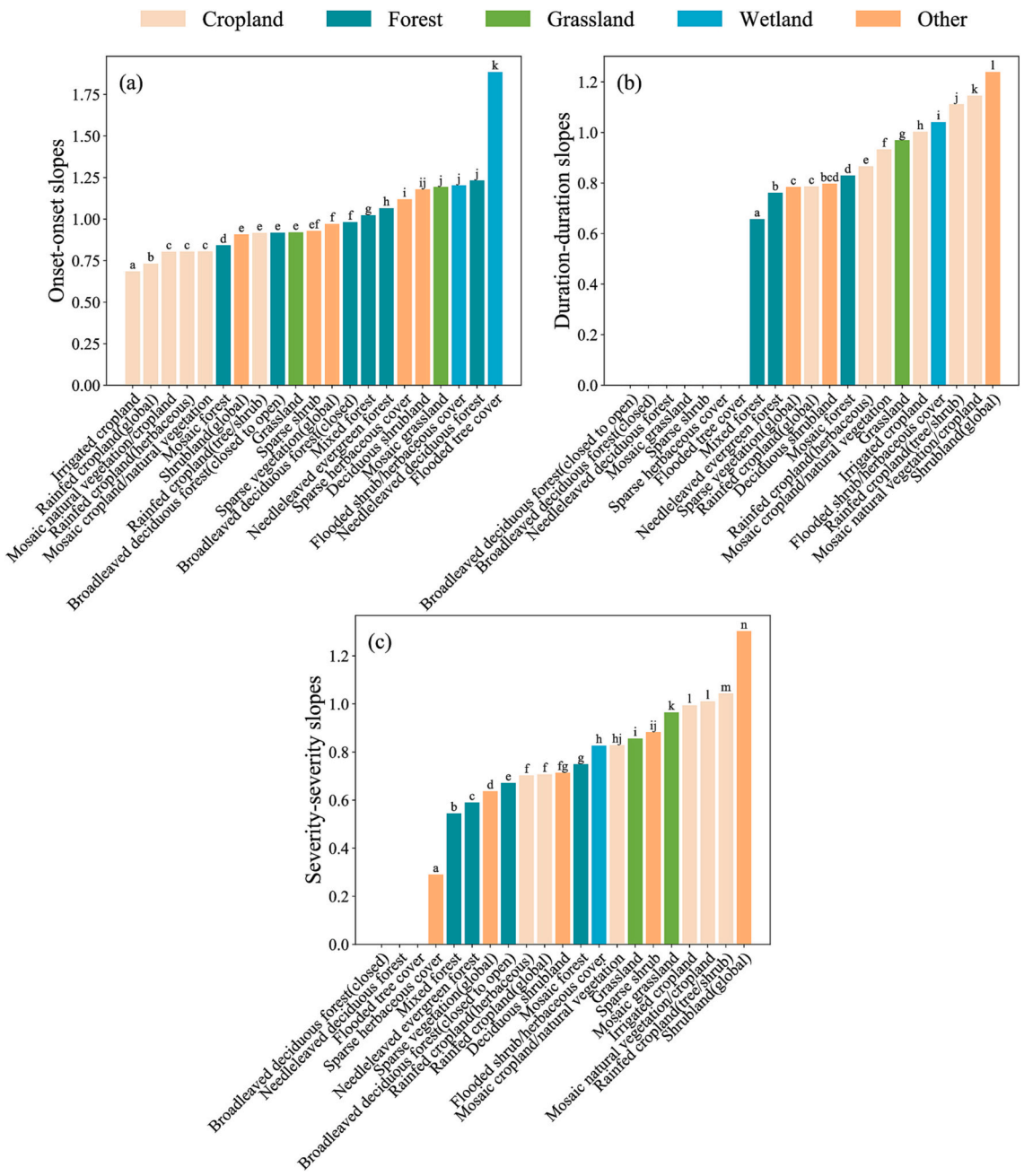

Fig. 2. Vulnerability varies between different ecosystems based on slopes derived from drought and vegetation damage characteristics. a–c: Slopes in different ecosystem types derived for onset-onset (**a**), duration-duration (**b**), and severity-severity (**c**) relationships of drought vs damage in ecosystem cover based on standardized major axis (SMA) models. The letters above the slopes bars indicate which ecosystem types differ significantly in their slopes, with the same letter meaning similar slopes. The color of the bars represents different ecosystem type categories. Please note that insignificant slopes ($p > 0.05$) and slopes with low correlation ($R^2 < 0.01$) are not shown.

not show a strong relationship between drought severity and vegetation damage severity (severity-severity slopes not shown in Fig. 2c). Their low sensitivity to drought severity variation is also apparent in Fig. 3.

3.3. *Vulnerability changes disproportionally with drought severity*

The previous sections showed strong differences among ecosystem types in their vulnerability to drought with relatively similar differences in vulnerabilities between ecosystem types for the different drought metrics. Onset and duration primarily relate to phenology impacts, while severity ultimately relates to many ecosystem functions. To understand how vulnerability changes with increasing drought severity, we evaluated the severity-severity slopes for varying drought severity based on first derivatives from generalized additive model (GAM).

Most ecosystem types showed increasing damage vulnerability as the severity of drought increases (Fig. 4). This accelerating trend, however, declines when vegetation damage has reached high levels under severe drought. This pattern was most strongly found for severity-severity slope changes and to some extent also for duration-duration slopes. The onset-onset slope did not show consistent changes with increasing drought. These results also indicate that with increasing drought severity under climate change (Vicente-Serrano et al., 2014), vegetation damage could increase disproportionally for most ecosystem types. This disproportional response suggests that as drought intensifies in the coming

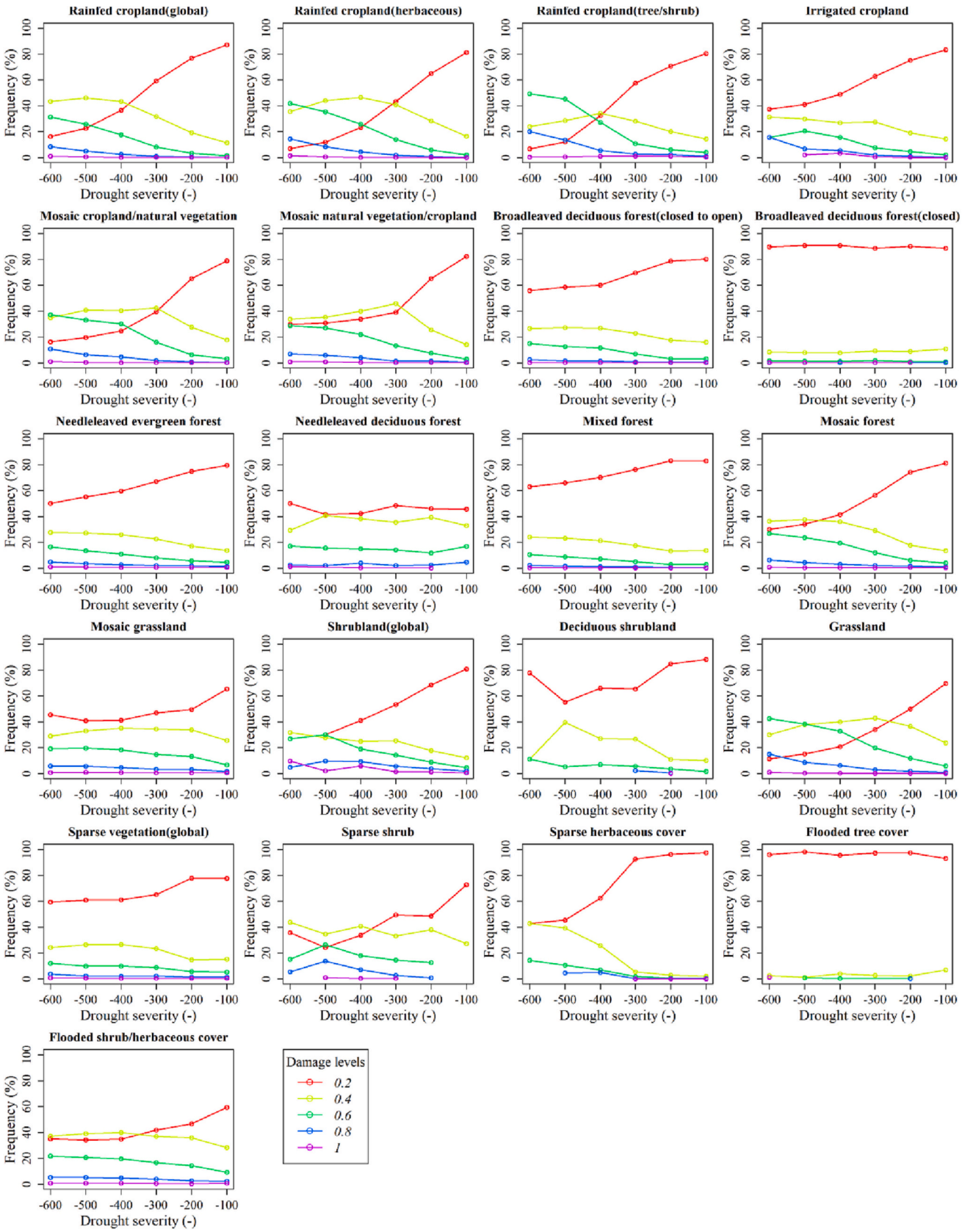

Fig. 3. Distribution of vegetation damage with drought severity. Lines represent the percentage of observations of a given damage level for each drought severity level. Colors represent each of the 5 damage levels.

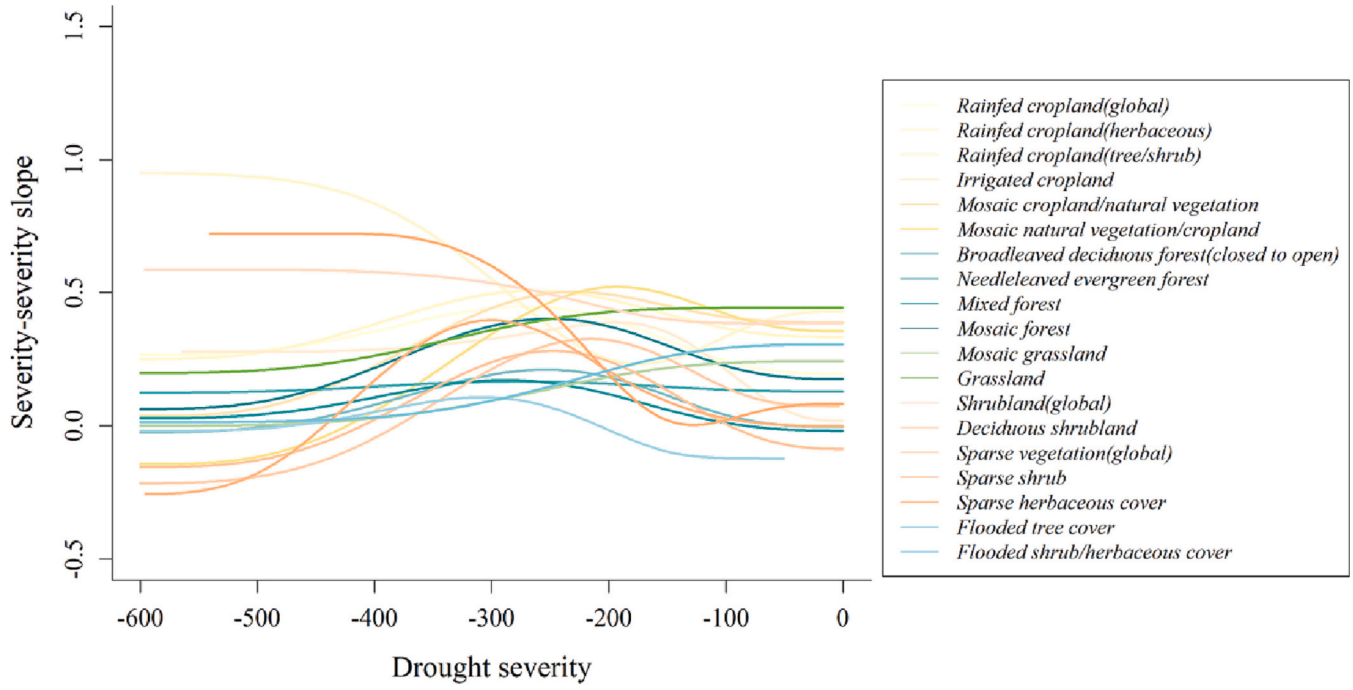

Fig. 4. Severity-severity slopes with increasing drought severity for various ecosystem types. The monochromatic color of the lines represents different ecosystem categories (as defined in Fig. 2).

decades, the performance of a wide range of ecosystem types will be threatened.

4. Discussion

4.1. Vulnerability variation between and within ecosystem types

With drought severity and duration going to increase in many regions under climate change, knowing how ecosystems will respond to those drought characteristics of recurrent drought is crucial. By quantifying ecosystem vulnerability (from onset-onset, duration-duration and severity-severity slopes) at a high-resolution, we provide a holistic perspective to ecosystem vulnerability. We observed that the differences in vulnerability depend mainly on ecosystem type instead of on location. Different ecosystem types located in the same area showing various response patterns, while ecosystem types that are widely distributed in Europe showed consistent responses.

In particular we observed that most forest ecosystems show low vulnerability with high buffering capacity to intensified drought. They suffered less drought impact under water stress, this is consistent with previous studies (Nicolai-Shaw et al., 2017; Páscoa et al., 2020) and is likely attributed to their deep root systems. However, between forests, still major differences are found. Our results for broadleaved deciduous forests showed a relatively faster response and higher damage vulnerability than for needle-leaved evergreen forests and mixed forests. Most likely, this is because the strategy of broadleaved deciduous trees is to reduce the leaf area in order to protect themselves against the hydraulic damage under drought (Bréda et al., 2006; Munné-Bosch and Alegre, 2004; Schuldt, 2020). Needleleaved forests showed the slowest response among all forests, which may be explained by their water saving strategy, with wide hydraulic safety margins, early stomatal closure and lower carbon gain (Carnicer et al., 2013; Choat et al., 2012). Mixed forests showed a lower vulnerability than needle-leaved evergreen forests and broadleaved deciduous forests. A possible explanation for this is that a mixed forest represents different (broad-leaved and coniferous) compensating strategies to deal with drought as related to their different physiological traits (Anderegg and Hillerislambers, 2016; Migliavacca et al., 2021; Pardos et al., 2021). Broad-leaved trees generally show a larger latent heat flux due to higher stomatal conductance, which could cool the mixed forest during drought, but will increase the risk of soil moisture scarcity at the same time (Schwaab et al., 2020).

In addition to forests, also wetlands – and particularly forested wetlands – showed very long delay times and low responses to drought duration and severity (Fig. 2). In the case of wetlands, this is likely related to the large water buffering capacity of wetlands that is not accounted for in the SPEI characterization of drought. In contrast, we observed that croplands were generally highly vulnerable to drought impacts, which may be related to the generally lower resistance of agricultural systems compared to natural ecosystems (De Keersmaecker et al., 2016).

Despite the clear differences between ecosystem types, we also observed large variations in vegetation damage severity in response to drought severity within different ecosystem types (Supplementary Fig. S6). This variation may be derived from either differences in vegetation strategies of the various plant species within an ecosystem type, or from different soil conditions, such as available soil-water-retention and soil fertility across different locations (Rita et al., 2020). Indeed, soil characteristics have been found to impact angiosperm resistance in dry or wet seasons (Li et al., 2020). Likewise, soil microbial presence has been shown to increase drought resistance of some plants or ameliorate drought stress in plants (Kannenberg and Phillips, 2017; Xi et al., 2018). Further studies of these variations are needed to achieve more accurate drought impact prediction.

The variation in duration-duration patterns (supplementary Fig. S5) within some ecosystem types was larger than that of severity-severity patterns, while the variation in onset-onset patterns (supplementary Fig. S4) between and within ecosystem types was found to be much lower. Most onsets have a slope around one, suggesting a tight and robust relationship between drought onset and vegetation damage onset. This coupling is even stronger for agricultural ecosystems than for other ecosystem types. Moreover, while there is a certain association between the onsets of vegetation damage and drought, we find little impact of the drought onset on the total vegetation damage under similar drought conditions, indicating that the vulnerability does not

strongly depend on the timing (early or late during the growing season) of the drought. In combination, our evidence therefore indicates that drought severity might be among the more critical metrics for estimating future drought impacts on vegetation.

4.2. A disproportionally increased vulnerability to intensified drought

Although there is major variation in the vulnerability within individual ecosystem types, in general, the vulnerability of most ecosystem types tends to increase rapidly once drought begins to become severe. In this context, even a slight increase in drought severity may lead to nonlinear effects through increased mortality risks. As drought severity increases, ecosystems reach high levels of vulnerability, although the drought severity at which maximum levels of vulnerability are reached varies between ecosystem types. This implies that under severe drought situations, even drought-tolerant ecosystems can hardly avoid being severely impaired by drought. It also suggests that with increasing drought severity under climate change, ecosystems are more likely to become highly vulnerable and may collapse. Therefore, a vast range of ecosystem types is threatened by the intensified drought in the future.

4.3. Implications for future climate change adaptation

Our ecosystem vulnerability results provide useful information for upcoming climatological challenges. Diversity in species, traits and functional strategies to drought has been acknowledged as important factors in regulating the vulnerability of ecosystems to drought (Anderegg et al., 2018; Grossiord, 2020). We found that mixed forests with their higher diversity have lower vulnerability than monospecific forests during drought. Increasing drought severity in future climate can further affect forest structures and functions, and thus carbon cycling and its feedback to the climate system (Frank et al., 2015). Forest management strategies aiming to increase diversity within forests may help to increase the resistance of the whole forest ecosystem to drought and thus reduce the negative impacts of drought on carbon cycling. Thus, managing carbon sequestration and storage in the future requires careful consideration of forest vulnerability.

With regard to agricultural production in a changing climate, we found that irrigated croplands are particularly vulnerable with low buffering capacity when facing intensified drought and much more vulnerable than rainfed croplands. A possible explanation for this is that irrigated crops usually need large amounts and constant water supply, and a shortage of irrigation during severe drought will cause water stress, to which some of them lack strategies to adapt. Considering that irrigated crops have yields at least twice those of nearby rainfed crops and that irrigated agriculture accounts for nearly half (47%) of all crop production in developing countries (Dubois et al., 2011), this could potentially have severe implications on global food insecurity. In line with a projected increase in droughts frequency, yields of irrigated crops may be threatened further, and the pressure on water resources due to irrigation will further increase. Hence, advanced deployment and planning of water resources or development of recycled water technology, improvements of crop drought tolerance and diversification in the food system (IPCC, 2019) are needed to reduce risks.

Flooded shrub and herbaceous cover showed a long delay time to drought, while the damage vulnerability of herbaceous cover and shrubs in wetlands is only slightly less than that of terrestrial grasslands. Some non-woody wetland vegetation may quickly recover under re-wetting conditions after drought through seed germination or rhizome regeneration. However, the extent to which recovery will occur depends on the water availability after the drought (Capon and Reid, 2016). With increasing shortage in the future, the wetland environment is facing the risk of degradation (Sandi et al., 2020). Therefore, the management and protection of the wetland vegetation are also important. Woody vegetation is not as adaptable as herbaceous cover in relatively arid or harsh environments (e.g. in ecosystems with sparse vegetation and in rainfed croplands). Under extreme drought conditions, these woody vegetations may further degenerate or experience the invasion of exotic shrub/herbaceous species (Caldeira et al., 2015; Puritty et al., 2019).

5. Conclusion

Our continental-scale analysis shows that ecosystems differ in their vulnerability to deteriorating drought conditions. In particular, irrigated croplands showed the shortest delay in response to drought (0.67 times that of other ecosystems) and a fast increase in damage to drought (1.27 times that of other ecosystems). Thus, they are considered at extremely high risk when facing future drought and mitigation activities are needed to reduce these risks. Among all ecosystems, mixed forests showed a very low vulnerability with a high buffering capacity against the increasing drought conditions. Their damage increased more slowly with drought, 0.67 times that of other ecosystems and 0.81 times that of other forests. Increasing diversity within forests may help to increase the drought resistance of entire forest ecosystems and thus to reduce drought impacts on the global carbon balance. Moreover, most ecosystem types tend to show an increasing vulnerability to intensified droughts, which suggests that a vast range of ecosystems is at risk under climate change. The multi-faceted assessment of ecosystem vulnerability provided in our study will help to forecast and quantify vegetation damage to future global climate change challenges and inform drought mitigation policies.

Code availability

All data and code used for the analysis are available on request from the corresponding author.

Credit author statement

P.V.B. directed the research. P.V.B., J.T. and Q.C. designed the research. Q.C. performed the analysis with inputs from P.V.B., J.T. and W.W. The results were interpreted by P.V.B., J.T. and Q.C. Q.C. wrote the first draft of the paper with revision from P.V.B., J.T.

Declaration of Competing Interest

The authors declare that they have no known competing financial interests or personal relationships that could have appeared to influence the work reported in this paper.

Data availability

All data used in this study are publicly available. JRC MARS precipitation data are available at http://data.europa.eu/89h/jrc-marsop4-7-weather_obs_grid_2019; The Meteosat Second Generation-Cloud Physical Properties (MSG-CPP) precipitation data are available at https://msgcpp.knmi.nl; MODIS MOD16A2 PET data are available at https://doi.org/10.5067/MODIS/MOD16A2.006; GEOV2 LAI data are available at https://land.copernicus.eu/global/products/lai; NASA Earth Observations fire data are available at https://neo.gsfc.nasa.gov/; Copernicus Climate Change Service (C3S) 2018 landcover (LC) map are available at https://cds.climate.copernicus.eu/cdsapp#!/dataset/satellite-land-cover?tab=overview; Modis phenology data are available at https://doi.org/10.5067/VIIRS/VNP22Q2.001.

Acknowledgements

We acknowledge the Copernicus Service Information (2019) for providing LAI data. We also acknowledge the ESA CCI Land Cover and the EC C3S Land Cover project for providing landcover map. Qi Chen is grateful to support from the China Scholarship Council (Grant No. 201806810030).

Appendix A. Supplementary data

Supplementary data to this article can be found online at https://doi.org/10.1016/j.rse.2023.113512.

References

AghaKouchak, A., Farahmand, A., Melton, F.S., Teixeira, J., Anderson, M.C., Wardlow, B. D., Hain, C.R., 2015. Remote sensing of drought: progress, challenges and opportunities. Rev. Geophys. 53, 452–480. https://doi.org/10.1002/2014RG000456.

Allen, C.D., Macalady, A.K., Chenchouni, H., Bachelet, D., McDowell, N., Vennetier, M., Kitzberger, T., Rigling, A., Breshears, D.D., Hogg, E.H.Ted, Gonzalez, P., Fensham, R., Zhang, Z., Castro, J., Demidova, N., Lim, J.H., Allard, G., Running, S. W., Semerci, A., Cobb, N., 2010. A global overview of drought and heat-induced tree mortality reveals emerging climate change risks for forests. For. Ecol. Manage. 259, 660–684. https://doi.org/10.1016/J.FORECO.2009.09.001.

Anderegg, L.D.L., Hillerislambers, J., 2016. Drought stress limits the geographic ranges of two tree species via different physiological mechanisms. Glob. Chang. Biol. 22, 1029–1045. https://doi.org/10.1111/GCB.13148.

Anderegg, W.R.L., Kane, J.M., Anderegg, L.D.L., 2013. Consequences of widespread tree mortality triggered by drought and temperature stress. Nat. Clim. Chang. 3, 30–36. https://doi.org/10.1038/nclimate1635.

Anderegg, W.R.L., Konings, A.G., Trugman, A.T., Yu, K., Bowling, D.R., Gabbitas, R., Karp, D.S., Pacala, S., Sperry, J.S., Sulman, B.N., Zenes, N., 2018. Hydraulic diversity of forests regulates ecosystem resilience during drought. Nature. 561, 538–541. https://doi.org/10.1038/s41586-018-0539-7.

Anderegg, W.R.L., Trugman, A.T., Bowling, D.R., Salvucci, G., Tuttle, S.E., 2019. Plant functional traits and climate influence drought intensification and land–atmosphere feedbacks. Proc. Natl. Acad. Sci. U. S. A. 116, 14071–14076. https://doi.org/10.1073/PNAS.1904747116/-/DCSUPPLEMENTAL.

Batllori, E., Lloret, F., Aakala, T., Anderegg, W.R.L., Aynekulu, E., Bendixsen, D.P., Bentouati, A., Bigler, C., Burk, C.J., Camarero, J.J., Colangelo, M., Coop, J.D., Fensham, R., Floyd, M.L., Galiano, L., Ganey, J.L., Gonzalez, P., Jacobsen, A.L., Kane, J.M., Kitzberger, T., Linares, J.C., Marchetti, S.B., Matusick, G., Michaelia, M., Navarro-Cerrillo, R.M., Pratt, R.B., Redmond, M.D., Rigling, A., Ripullone, F., Sangüesa-Barreda, G., Sasal, Y., Saura-Mas, S., Suarez, M.L., Veblen, T.T., Vilà-Cabrera, A., Vincke, C., Zeeman, B., 2020. Forest and woodland replacement patterns following drought-related mortality. Proc. Natl. Acad. Sci. U. S. A. 117, 29720–29729. https://doi.org/10.1073/pnas.2002314117.

Bréda, N., Huc, R., Granier, A., Dreyer, E., 2006. Temperate forest trees and stands under severe drought: a review of ecophysiological responses, adaptation processes and long-term consequences. Ann. For. Sci. 63, 625–644.

Büntgen, U., Urban, O., Krusic, P.J., Rybníček, M., Kolář, T., Kyncl, T., Ač, A., Koňasová, E., Čáslavský, J., Esper, J., Wagner, S., Saurer, M., Tegel, W., Dobrovolný, P., Cherubini, P., Reinig, F., Trnka, M., 2021. Recent European drought extremes beyond common era background variability. Nat. Geosci. 14, 190–196. https://doi.org/10.1038/s41561-021-00698-0.

C3S, 2019. Land cover classification gridded maps from 1992 to present derived from satellite observations. . Available at: https://cds.climate.copernicus.eu/cdsapp#!/dataset/satellite-land-cover?tab=overview.

Caldeira, M.C., Lecomte, X., David, T.S., Pinto, J.G., Bugalho, M.N., Werner, C., 2015. Synergy of extreme drought and shrub invasion reduce ecosystem functioning and resilience in water-limited climates. Sci. Rep. 5, 1–9. https://doi.org/10.1038/srep15110.

Capon, S.J., Reid, M.A., 2016. Vegetation resilience to mega-drought along a typical floodplain gradient of the southern Murray-Darling Basin, Australia. J. Veg. Sci. 27, 926–937. https://doi.org/10.1111/jvs.12426.

Carnicer, J., Barbeta, A., Sperlich, D., Coll, M., Penuelas, J., 2013. Contrasting trait syndromes in angiosperms and conifers are associated with different responses of tree growth to temperature on a large scale. Front. Plant Sci. 4 https://doi.org/10.3389/fpls.2013.00409.

Chen, Q., Timmermans, J., Wen, W., van Bodegom, P.M., 2022. A multi-metric assessment of drought vulnerability across different vegetation types using high resolution remote sensing. Sci. Total Environ. https://doi.org/10.1016/J.SCITOTENV.2022.154970.

Choat, B., Jansen, S., Brodribb, T.J., Cochard, H., Delzon, S., Bhaskar, R., Bucci, S.J., Feild, T.S., Gleason, S.M., Hacke, U.G., Jacobsen, A.L., Lens, F., Maherali, H., Martínez-Vilalta, J., Mayr, S., Mencuccini, M., Mitchell, P.J., Nardini, A., Pittermann, J., Pratt, R.B., Sperry, J.S., Westoby, M., Wright, I.J., Zanne, A.E., 2012. Global convergence in the vulnerability of forests to drought. Nature. 491, 752–755. https://doi.org/10.1038/NATURE11688.

Ciais, P., Reichstein, M., Viovy, N., Granier, A., Ogée, J., Allard, V., Aubinet, M., Buchmann, N., Bernhofer, C., Carrara, A., Chevallier, F., De Noblet, N., Friend, A.D., Friedlingstein, P., Grünwald, T., Heinesch, B., Keronen, P., Knohl, A., Krinner, G., Loustau, D., Manca, G., Matteucci, G., Miglietta, F., Ourcival, J.M., Papale, D., Pilegaard, K., Rambal, S., Seufert, G., Soussana, J.F., Sanz, M.J., Schulze, E.D., Vesala, T., Valentini, R., 2005. Europe-wide reduction in primary productivity caused by the heat and drought in 2003. Nature 437, 529–533. https://doi.org/10.1038/nature03972.

Copernicus Service Information, 2019. Leaf Area Index.. Available at: https://land.copernicus.eu/global/products/lai.

De Keersmaecker, W., van Rooijen, N., Lhermitte, S., Tits, L., Schaminée, J., Coppin, P., Honnay, O., Somers, B., 2016. Species-rich semi-natural grasslands have a higher resistance but a lower resilience than intensively managed agricultural grasslands in response to climate anomalies. J. Appl. Ecol. 53, 430–439. https://doi.org/10.1111/1365-2664.12595.

Ding, Y., Xu, J., Wang, X., Peng, X., Cai, H., 2020. Spatial and temporal effects of drought on Chinese vegetation under different coverage levels. Sci. Total Environ. 716, 137166 https://doi.org/10.1016/j.scitotenv.2020.137166.

Dubois, O., et al., 2011. The state of the world's land and water resources for food and agriculture: managing systems at risk. Earthscan.

Field, C.B., Barros, V., Stocker, T.F., Dahe, Q., Jon Dokken, D., Ebi, K.L., Mastrandrea, M. D., Mach, K.J., Plattner, G.K., Allen, S.K., Tignor, M., Midgley, P.M., 2012. Managing the Risks of Extreme Events and Disasters to Advance Climate Change Adaptation: Special Report of the Intergovernmental Panel on Climate Change. In: Cambridge University Press. https://doi.org/10.1017/CBO9781139177245.

Frank, Dorothea, Reichstein, M., Bahn, M., Thonicke, K., Frank, David, Mahecha, M.D., Smith, P., van der Velde, M., Vicca, S., Babst, F., Beer, C., Buchmann, N., Canadell, J. G., Ciais, P., Cramer, W., Ibrom, A., Miglietta, F., Poulter, B., Rammig, A., Seneviratne, S.I., Walz, A., Wattenbach, M., Zavala, M.A., Zscheischler, J., 2015. Effects of climate extremes on the terrestrial carbon cycle: concepts, processes and potential future impacts. Glob. Chang. Biol. 21, 2861–2880. https://doi.org/10.1111/GCB.12916.

Gouveia, C.M., Trigo, R.M., Beguería, S., Vicente-Serrano, S.M., 2017. Drought impacts on vegetation activity in the Mediterranean region: an assessment using remote sensing data and multi-scale drought indicators. Glob. Planet. Change 151, 15–27. https://doi.org/10.1016/j.gloplacha.2016.06.011.

Grossiord, C., 2020. Having the right neighbors: how tree species diversity modulates drought impacts on forests. New Phytol. 228, 42–49. https://doi.org/10.1111/NPH.15667.

Gupta, A., Rico-Medina, A., Caño-Delgado, A.I., 2020. The physiology of plant responses to drought. Science 368, 266–269. https://doi.org/10.1126/science.aaz7614.

Huete, A., Didan, K., Miura, T., Rodriguez, E.P., Gao, X., Ferreira, L.G., 2002. Overview of the radiometric and biophysical performance of the MODIS vegetation indices. Remote Sens. Environ. 83, 195–213. https://doi.org/10.1016/S0034-4257(02)00096-2.

IPCC, 2019. Climate Change and Land: an IPCC special report on climate change, desertification, land degradation, sustainable land management, food security, and greenhouse gas fluxes in terrestrial ecosystems.

Ji, L., Peters, A.J., 2003. Assessing vegetation response to drought in the northern Great Plains using vegetation and drought indices. Remote Sens. Environ. 87, 85–98. https://doi.org/10.1016/S0034-4257(03)00174-3.

Jönsson, P., Eklundh, L., 2004. TIMESAT—a program for analyzing time-series of satellite sensor data. Comput. Geosci. 30, 833–845. https://doi.org/10.1016/J.CAGEO.2004.05.006.

Jönsson, P., Eklundh, L., 2002. Seasonality extraction by function fitting to time-series of satellite sensor data. IEEE Trans. Geosci. Remote Sens. 40, 1824–1832. https://doi.org/10.1109/TGRS.2002.802519.

Kang, H., Sridhar, V., Mainuddin, M., Trung, L.D., 2021. Future rice farming threatened by drought in the lower Mekong Basin. Sci. Rep. 11, 9383. https://doi.org/10.1038/s41598-021-88405-2.

Kannenberg, S.A., Phillips, R.P., 2017. Soil microbial communities buffer physiological responses to drought stress in three hardwood species. Oecologia 183, 631–641. https://doi.org/10.1007/s00442-016-3783-2.

Kogan, F.N., 1995. Droughts of the late 1980s in the United States as Derived from NOAA polar-orbiting satellite data. Bull. Am. Meteorol. Soc. 76, 655–668. https://doi.org/10.1175/1520-0477(1995)076<0655:dotlit>2.0.co;2.

Kuenzer, C., Ottinger, M., Wegmann, M., Guo, H., Wang, C., Zhang, J., Dech, S., Wikelski, M., 2014. Earth observation satellite sensors for biodiversity monitoring: potentials and bottlenecks. Int. J. Remote Sens. https://doi.org/10.1080/01431161.2014.964349.

Li, X., Piao, S., Wang, K., Wang, X., Wang, T., Ciais, P., Chen, A., Lian, X., Peng, S., Peñuelas, J., 2020. Temporal trade-off between gymnosperm resistance and resilience increases forest sensitivity to extreme drought. Nat. Ecol. Evol. 4, 1075–1083. https://doi.org/10.1038/s41559-020-1217-3.

McKee, T.B., Doesken, N.J., Kleist, J., 1993. In: The relationship of drought frequency and duration to time scales. American Meteorological Society, Boston, MA, pp. 179–183.

Migliavacca, M., Musavi, T., Mahecha, M.D., Nelson, J.A., Knauer, J., Baldocchi, D.D., Perez-Priego, O., Christiansen, R., Peters, J., Anderson, K., Bahn, M., Black, T.A., Blanken, P.D., Bonal, D., Buchmann, N., Caldararu, S., Carrara, A., Carvalhais, N., Cescatti, A., Chen, J., Cleverly, J., Cremonese, E., Desai, A.R., El-Madany, T.S., Farella, M.M., Fernández-Martínez, M., Filippa, G., Forkel, M., Galvagno, M., Gomarasca, U., Gough, C.M., Göckede, M., Ibrom, A., Ikawa, H., Janssens, I.A., Jung, M., Kattge, J., Keenan, T.F., Knohl, A., Kobayashi, H., Kraemer, G., Law, B.E., Liddell, M.J., Ma, X., Mammarella, I., Martini, D., Macfarlane, C., Matteucci, G., Montagnani, L., Pabon-Moreno, D.E., Panigada, C., Papale, D., Pendall, E., Penuelas, J., Phillips, R.P., Reich, P.B., Rossini, M., Rotenberg, E., Scott, R.L., Stahl, C., Weber, U., Wohlfahrt, G., Wolf, S., Wright, I.J., Yakir, D., Zaehle, S., Reichstein, M., 2021. The three major axes of terrestrial ecosystem function. Nature 598, 468–472. https://doi.org/10.1038/s41586-021-03939-9.

Millar, C.I., Stephenson, N.L., 2015. Temperate forest health in an era of emerging megadisturbance. Science 349, 823–826. https://doi.org/10.1126/science.aaa9933.

Muffler, L., Weigel, R., Hacket-Pain, A.J., Klisz, M., van der Maaten, E., Wilmking, M., Kreyling, J., van der Maaten-Theunissen, M., 2020. Lowest drought sensitivity and decreasing growth synchrony towards the dry distribution margin of European beech. J. Biogeogr. 47, 1910–1921. https://doi.org/10.1111/JBI.13884.

Munné-Bosch, S., Alegre, L., 2004. Die and let live: leaf senescence contributes to plant survival under drought stress. Funct. Plant Biol. https://doi.org/10.1071/FP03236.

Naumann, G., Cammalleri, C., Mentaschi, L., Feyen, L., 2021. Increased economic drought impacts in Europe with anthropogenic warming. Nat. Clim. Chang. 11, 485–491. https://doi.org/10.1038/s41558-021-01044-3.

Nicolai-Shaw, N., Zscheischler, J., Hirschi, M., Gudmundsson, L., Seneviratne, S.I., 2017. A drought event composite analysis using satellite remote-sensing based soil moisture. Remote Sens. Environ. 203, 216–225. https://doi.org/10.1016/j.rse.2017.06.014.

Palmer, W.C., 1965. Meteorological Drought. U.S. Weather Bur. Res. Pap. No. 45.

Pardos, M., del Río, M., Pretzsch, H., Jactel, H., Bielak, K., Bravo, F., Brazaitis, G., Defossez, E., Engel, M., Godvod, K., Jacobs, K., Jansone, L., Jansons, A., Morin, X., Nothdurft, A., Oreti, L., Ponette, Q., Pach, M., Riofrío, J., Ruíz-Peinado, R., Tomao, A., Uhl, E., Calama, R., 2021. The greater resilience of mixed forests to drought mainly depends on their composition: analysis along a climate gradient across Europe. For. Ecol. Manag. 481, 118687 https://doi.org/10.1016/J.FORECO.2020.118687.

Páscoa, P., Gouveia, C.M., Russo, A.C., Bojariu, R., Vicente-Serrano, S.M., Trigo, R.M., 2020. Drought impacts on vegetation in southeastern Europe. Remote Sens. 12, 2156. https://doi.org/10.3390/rs12132156.

Páscoa, P., Gouveia, C.M., Russo, A.C., Bojariu, R., Vicente-Serrano, S.M., Trigo, R.M., 2018. Vegetation vulnerability to drought on southeastern Europe. Hydrol. Earth Syst. Sci. Discuss. 2018, 1–29. https://doi.org/10.5194/hess-2018-264.

Phillips, O.L., Aragão, L.E.O.C., Lewis, S.L., Fisher, J.B., Lloyd, J., López-González, G., Malhi, Y., Monteagudo, A., Peacock, J., Quesada, C.A., Van Der Heijden, G., Almeida, S., Amaral, I., Arroyo, L., Aymard, G., Baker, T.R., Bánki, O., Blanc, L., Bonal, D., Brando, P., Chave, J., De Oliveira, Á.C.A., Cardozo, N.D., Czimczik, C.I., Feldpausch, T.R., Freitas, M.A., Gloor, E., Higuchi, N., Jiménez, E., Lloyd, G., Meir, P., Mendoza, C., Morel, A., Neill, D.A., Nepstad, D., Patiño, S., Peñuela, M.C., Prieto, A., Ramírez, F., Schwarz, M., Silva, J., Silveira, M., Thomas, A.S., Steege, H. Ter, Stropp, J., Vásquez, R., Zelazowski, P., Dávila, E.A., Andelman, S., Andrade, A., Chao, K.J., Erwin, T., Di Fiore, A., Honorio, E.C., Keeling, H., Killeen, T.J., Laurance, W.F., Cruz, A.P., Pitman, N.C.A., Vargas, P.N., Ramírez-Angulo, H., Rudas, A., Salamão, R., Silva, N., Terborgh, J., Torres-Lezama, A., 2009. Drought sensitivity of the amazon rainforest. Science 323, 1344–1347. https://doi.org/10.1126/science.1164033.

Puritty, C.E., Esch, E.H., Castro, S.P., Ryan, E.M., Lipson, D.A., Cleland, E.E., 2019. Drought in Southern California coastal sage scrub reduces herbaceous biomass of exotic species more than native species, but exotic growth recovers quickly when drought ends. Plant Ecol. 220, 151–169. https://doi.org/10.1007/s11258-019-00912-5.

Reichstein, M., Bahn, M., Ciais, P., Frank, D., Mahecha, M.D., Seneviratne, S.I., Zscheischler, J., Beer, C., Buchmann, N., Frank, D.C., Papale, D., Rammig, A., Smith, P., Thonicke, K., Van Der Velde, M., Vicca, S., Walz, A., Wattenbach, M., 2013. Climate extremes and the carbon cycle. Nature 500, 287–295. https://doi.org/10.1038/nature12350.

Rita, A., Camarero, J.J., Nolè, A., Borghetti, M., Brunetti, M., Pergola, N., Serio, C., Vicente-Serrano, S.M., Tramutoli, V., Ripullone, F., 2020. The impact of drought spells on forests depends on site conditions: the case of 2017 summer heat wave in southern Europe. Glob. Chang. Biol. 26, 851–863. https://doi.org/10.1111/GCB.14825.

Running, S., Mu, Q., Zhao, M., 2017. MOD16A2 MODIS/Terra Net Evapotranspiration 8-Day L4 Global 500m SIN Grid V006 [Data set]. NASA EOSDIS L. Process. DAAC. https://doi.org/10.5067/MODIS/MOD16A2.006.

Samaniego, L., Thober, S., Kumar, R., Wanders, N., Rakovec, O., Pan, M., Zink, M., Sheffield, J., Wood, E.F., Marx, A., 2018. Anthropogenic warming exacerbates european soil moisture droughts. Nat. Clim. Chang. 8, 421–426. https://doi.org/10.1038/s41558-018-0138-5.

Sandi, S.G., Rodriguez, J.F., Saintilan, N., Wen, L., Kuczera, G., Riccardi, G., Saco, P.M., 2020. Resilience to drought of dryland wetlands threatened by climate change. Sci. Rep. 10, 1–14. https://doi.org/10.1038/s41598-020-70087-x.

Schuldt, B., 2020. A first assessment of the impact of the extreme 2018 summer drought on Central European forests. Basic Appl. Ecol. https://doi.org/10.1016/j.baae.2020.04.003.

Schwaab, J., Davin, E.L., Bebi, P., Duguay-Tetzlaff, A., Waser, L.T., Haeni, M., Meier, R., 2020. Increasing the broad-leaved tree fraction in european forests mitigates hot temperature extremes. Sci. Rep. 10, 14153. https://doi.org/10.1038/s41598-020-71055-1.

Seddon, A.W.R., Macias-Fauria, M., Long, P.R., Benz, D., Willis, K.J., 2016. Sensitivity of global terrestrial ecosystems to climate variability. Nature. 531, 229–232. https://doi.org/10.1038/nature16986.

Senf, C., Buras, A., Zang, C.S., Rammig, A., Seidl, R., 2020. Excess forest mortality is consistently linked to drought across Europe. Nat. Commun. 11, 1–8. https://doi.org/10.1038/s41467-020-19924-1.

Stovall, A.E.L., Shugart, H., Yang, X., 2019. Tree height explains mortality risk during an intense drought. Nat. Commun. 10, 1–6. https://doi.org/10.1038/s41467-019-12380-6.

Sun, Q., Miao, C., Duan, Q., Ashouri, H., Sorooshian, S., Hsu, K.L., 2018. A review of global precipitation data sets: data sources, estimation, and intercomparisons. Rev. Geophys. 56, 79–107. https://doi.org/10.1002/2017RG000574.

Toreti, A., 2014. Gridded Agro-Meteorological Data in Europe. European Commission, Joint Research Centre (JRC) [Dataset]. PID:. http://data.europa.eu/89h/jrc-marsop4-7-weather_obs_grid_2019.

Verschuur, J., Li, S., Wolski, P., Otto, F.E.L., 2021. Climate change as a driver of food insecurity in the 2007 Lesotho-South Africa drought. Sci. Rep. 11, 1–9. https://doi.org/10.1038/s41598-021-83375-x.

Vicente-Serrano, S.M., Beguería, S., López-Moreno, J.I., 2010. A multiscalar drought index sensitive to global warming: the standardized precipitation evapotranspiration index. J. Clim. 23, 1696–1718. https://doi.org/10.1175/2009JCLI2909.1.

Vicente-Serrano, S.M., Lopez-Moreno, J.I., Beguería, S., Lorenzo-Lacruz, J., Sanchez-Lorenzo, A., García-Ruiz, J.M., Azorin-Molina, C., Morán-Tejeda, E., Revuelto, J., Trigo, R., Coelho, F., Espejo, F., 2014. Evidence of increasing drought severity caused by temperature rise in southern Europe. Environ. Res. Lett. 9, 044001 https://doi.org/10.1088/1748-9326/9/4/044001.

Warton, D.I., Duursma, R.A., Falster, D.S., Taskinen, S., 2012. SMATR 3-an R package for estimation and inference about allometric lines. Methods Ecol. Evol. 3, 257–259. https://doi.org/10.1111/j.2041-210X.2011.00153.x.

Wood, S.N., 2011. Fast stable restricted maximum likelihood and marginal likelihood estimation of semiparametric generalized linear models. J. RStat. Soc. Ser. B Stat. Methodol. 73, 3–36. https://doi.org/10.1111/j.1467-9868.2010.00749.x.

World Economic Forum, 2018. The global risks report 2018 - 13th edition, Geneva, Switserland.

Xi, N., Chu, C., Bloor, J.M.G., 2018. Plant drought resistance is mediated by soil microbial community structure and soil-plant feedbacks in a savanna tree species. Environ. Exp. Bot. 155, 695–701. https://doi.org/10.1016/j.envexpbot.2018.08.013.

Xu, H.Jie, Wang, X.Ping, Zhao, C.Yan, Yang, X.Mei, 2018. Diverse responses of vegetation growth to meteorological drought across climate zones and land biomes in northern China from 1981 to 2014. Agric. For. Meteorol. 262, 1–13. https://doi.org/10.1016/j.agrformet.2018.06.027.

Zhang, Q., Kong, D., Singh, V.P., Shi, P., 2017. Response of vegetation to different time-scales drought across China: spatiotemporal patterns, causes and implications. Glob. Planet. Change 152, 1–11. https://doi.org/10.1016/j.gloplacha.2017.02.008.

Zhang, X., Friedl, M., Henebry, G., 2020. VIIRS/NPP Land Cover Dynamics Yearly L3 Global 500m SIN Grid V001 [Dataset]. NASA EOSDIS Land Processes DAAC. https://doi.org/10.5067/VIIRS/VNP22Q2.001.